We combined our response to each referee's comments below:

Author's responses to reviewer's comments follow. A copy of the reviewer comment is given (with comment 'number') followed by a response (blue font).

Response to referee 1

1. General comment

The authors of this study present high-quality record of the atmospheric CH_4 mole fractions measured at three WMO/GAW stations in Korea: Anmyeondo (AMY), Jeju Gosan Suwolbong (JGS), and Ulleungdo (ULD). To confirm the data quality in detail, the authors evaluate the total measurement uncertainties at the three sites, which are less than GAW's compatibility goal for atmospheric CH_4 measurement (±2 ppb). Then, they investigate the characteristic features of the CH_4 variations by precisely analyzing the excess CH_4 mole fractions from the background variations, the diurnal cycles, the seasonal cycles, and the growth rates. From PSS analysis and the $^{13}CH_4$ isotopic data obtained at nearby site (TAP), they also discuss the temporal changes in the source region and the dominant source categories from a 5-year period of 2000-2006 to that of 2016-2020. Although I think the discussion based on the PSS and isotopic analyses have some problems, I believe that the data presented in this report are quite reliable and contribute to the global modeling studies especially for the CH_4 emission analysis from the east Asia.

I found that the paper contains material that should be published in Atmospheric Physics and Chemistry. However, I think that the authors should make more efforts to improve the manuscript as is suggested in followings before publication.

Thank you for your comments on the paper's value. We also appreciate your helpful comments to improve our manuscript. According to your specific comments and considerations, we revised our manuscript.

2. I'm not sure why the authors discuss in depth the influence of water vapor on the CRDS analyzer in Section 2.3 and 3.1. The CRDS analyzer provides dry CH_4 mole fraction by measuring the water vapor simultaneously. The study of Rella et al. (2013) revealed that the preliminary reduction of water vapor of sample air less than 1% allow CRDS analyzer to measure the CH_4 mole fraction within the level of GAW's compatibility goal (±2 ppb). The authors describe that the air samples are dried to −50C. I believe that the laboratory standard gases and working standard gases uses in this study are sufficiently dried (I think that the absolute dew points should be clarified in the text). In addition, if the air samples are dried by a cold trap of −50 C, the dilution effect is comparable to the reproducibility of the CRDS analyzer. Therefore, I think it would be better to simplify the description about H_2O influence on the CRDS measurement.

Agree. But we do not use the water correction function provided by CRDS since we believe that H_2O value also should be calibrated when we apply the correction algorism to our data and general water correction cannot be applied to each instrument in different environment. So we clarify this in the manuscript. Please see the answer of # 11.
Since WMO GAW community emphasize the importance of drying air and its bias, we would like to explain relevant information detailed to prove the quality of our data. Especially readers and data users can have questions about our working standards and its bias through propagating against laboratory standards. To remove this reservation, we dealt with our working standards very deeply in section 2.3.
On the other hand, though the measurement uncertainty from drying system is also

negligible (0.006 to 0.008 ppb in Table 3), this value can be important. It is because that the standard gas is injected not through the drying system and separately from samples. However, the reviewer also mentioned the air dried at −50 C and the biases are very small. Therefore, it can be less valuable to deal with this deeply as one of uncertainty factors. We would like to keep the explanations about working standards while simplifying about the measurement uncertainty.

P4 L20: Despite the Picarro provides built-in dry correction algorism, this is not applied to our data since generic water correction cannot be applied to each instrument in different environment. Though we dry our samples with this system, the biases resulted from the different H_2O values between samples and standards or working and laboratory standards are considered here. This is described in section 2.3 and 3.1.

P10 L25: U_{h2o} was computed from the differences in H_2O (%) between the ambient airstream through the drying system and standard gases injected directly, bypassing the drying system. An ideal measurement would be through the analysis of the standard gases and air samples after they pass through the same drying system (WMO, 2016). However, our drying efficiency was not constant, so we injected standard gases directly as a reference value of H_2O. Therefore we considered the CH_4 dilution offsets between working standards and sample air while estimating the uncertainty with a similar method using Eq.(1) in section 2.3. Hourly CH_4 dilution maximum offsets are up to 0.009 ppb at AMY, 0.006 ppb at JGS and 0.009 ppb at ULD from 2016 to 2020. This uncertainty term was smallest (0.006 to 0.008 ppb) among all uncertainty factors in the KMA network as indicating the sampled air has negligible biases through our drying system

3. I'm very curious about the diurnal cycles of the L3 hourly data. If the data selection method described in Section 2.4.2 effectively remove the local effect, there is no

statistically significant diurnal cycles in the L3 data. Such information would be useful to make the L3 data more reliable

We attached L3 hourly data through step 1 to 3 in 2020 for three stations here. The scale is different according to stations, but it can be confirmed that our selection method is reasonable. We also add these graphs in the supplementary as Figure S2 to demonstrate our method is reasonable.
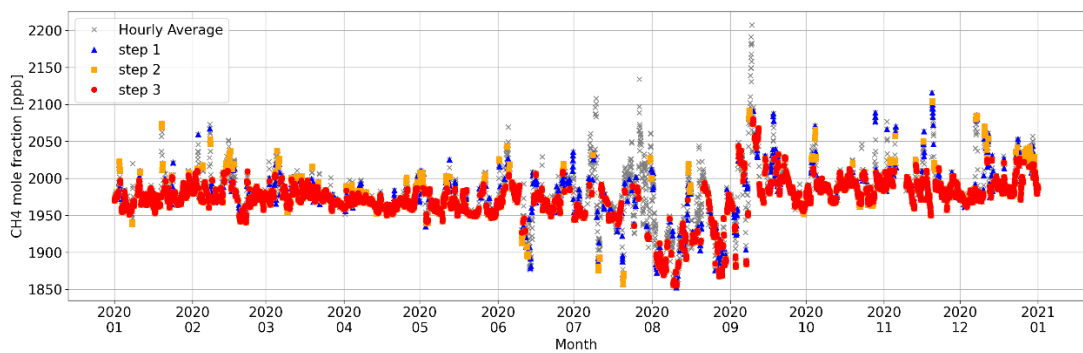
(a)
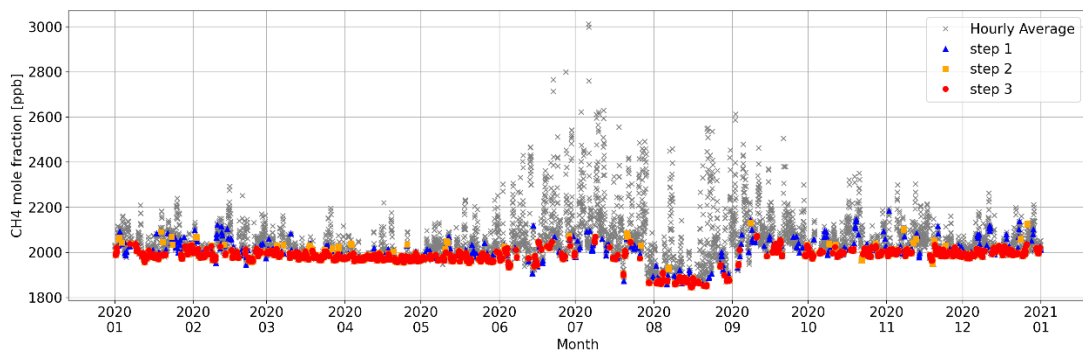
(b)
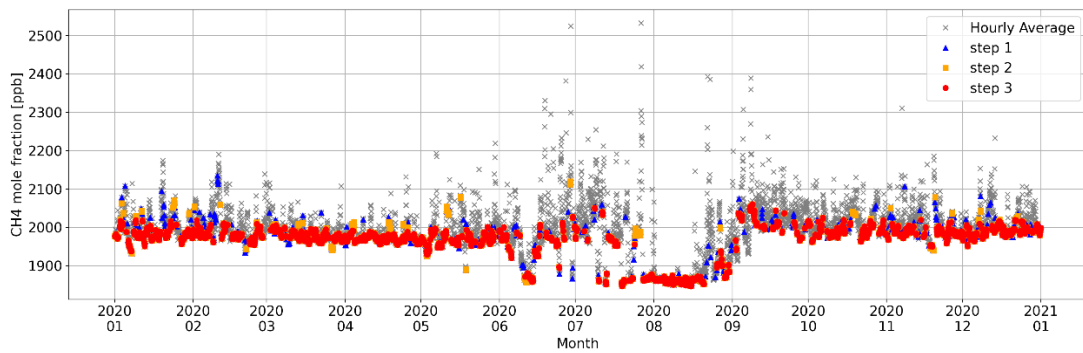
(c)

Figure A. The time series of hourly CH$_4$ data through our selection method from step 1 to 3 at (a) AMY (b) JGS and (c)ULD in 2020.

On the other hand, we also showed the L3 diurnal cycle at each station in 2020 here. As reviewer mentioned the diurnal cycle is almost flat within ±2 ppb variations regardless of stations. This variation might be resulted from the local meteorological effect by the radiation such as high boundary layer height in the daytime and stable in the night at least. Therefore, we have confidence that our L3 method remove local sink and source of CH$_4$.
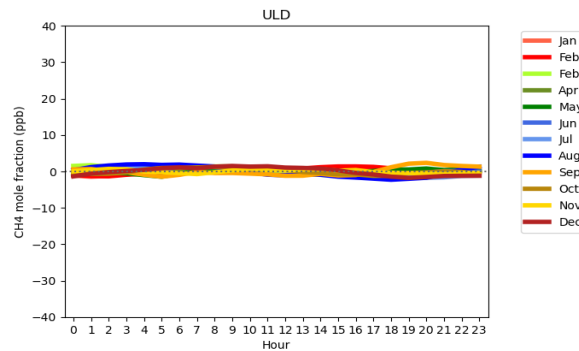
(a)
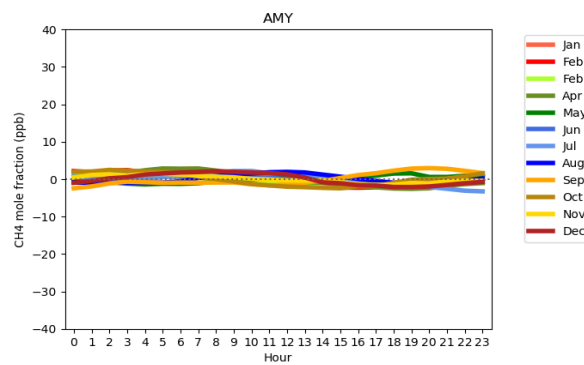
(b)
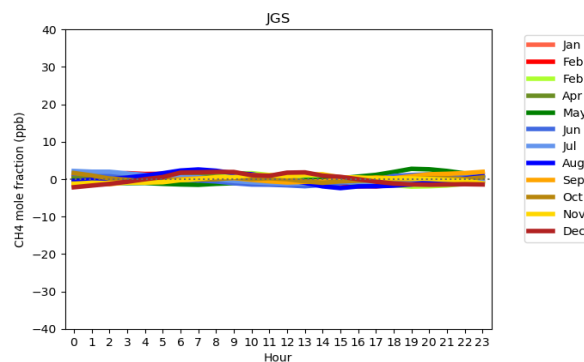
(c)

Figure B. Mean diurnal variations of CH_4. Values show the average departure from the daily mean in each month at (a) AMY and (b) JGS from 2016 to 2020 and (c) at ULD in 2020.

4. I don't agree with the discussion based on the PSS and the $\delta^{13}CH_4$ analyses in Section 3.5. As for the PSS analysis, I'm not sure how to interpret the plots shown in Figs 9a and 9b. Although the authors seem to consider that the plots reflect the CH_4 flux distributions, the flux distribution is considerably different from the previously reported flux distributions (e.g., Ito et al., 2019). Additionally, I cannot believe that such large temporal change in the flux distribution occurred between the two periods. So, I think that the authors should clarify what the plots based on the PSS analysis mean. The authors only show the plots based on the observation at AMY. But I'm curious about the similar plots based on the data at JGS and ULD. If the distributions based on JGS and ULD are similar to Fig. 9b, such result would convince us to some extent that the PSS analysis is reliable. I'm not sure what the isotopic analysis means. The authors would like to suggest that influences of the biogenic sources increased from 2006-2010 to 2016-2020 because the $\delta^{13}C_{(CH4)}$ values for the latter period shows faster decreasing rates than those for the former period. However, the background $\delta^{13}C_{(CH4)}$ data also show the secularly decreasing trend (for example, you can see the recent $\delta^{13}C_{(CH4)}$ change in NIWA's home page: https://niwa.co.nz/atmosphere/our-data/trace-gas-plots/methane). So, how do the authors distinguish the regional influence on the $\delta^{13}C_{(CH4)}$ values from

the background change? Additonally, why don't the authors use Miller-Tans plot to evaluate of the $\delta^{13}C$ values for the CH_4 regional sources? On the other hand, the values of the intercept of the Keeling plot for CS and KL increased from 2006-2010 to 2016-2020, suggesting the influence of the biogenic sources relatively decreased. This result is inconsistent with the above result. I'm also curious about the $\delta^{13}C_{(CH4)}$ data during the period from 2010 to 2016. Why don't the authors discuss the period from 2010 to 2016?

Thank you for the comment and we understand your considerations.

1) PSS analysis

For the PSS analysis, we described the detailed information in #20 and revised the section 2.7 with detailed descriptions.

When we analyze that ULD and JGS as well, the covered regions and CH_4xs scale were different due to observatory location (Please see Supplementary Figure S4). However, we confirmed that they indicated reasonably same areas as major source regions such as southern China and western Korea from 2016 to 2020. Therefore, we have a high confidence about PSS analysis. We also reviewed the Ito et al.(2019). Bottom-up approach cannot be exactly matched to PSS analysis since PSS analysis calculate the air-mass residence time-weighted mean concentrations not the CH_4 flux as we mentioned in revised section 2.7. This is the same reason that each stations showed slightly different coverage for the source regions in PSS analysis. PSS analysis only can give information which area potentially affect the atmospheric CH_4xs observed at each station.

On the other hand, what we would like to emphasize is CH_4 growth rate was driven by mixed source in East Asia while global by biogenic sources mainly. Therefore, we used PSS analysis as a tool to figure out representative source regions in East Asia and implicated the CH_4xs data from 2006 to 2020 (15 years). According to reviewer's suggestion, we analyzed Miller-Tans plots using the samples from source regions

thorough PSS analysis every 5 years period to see the source changes.

2) Isotope analysis

The reasons why we compare only between 2006/10 and 2016/2020, we would like to show the certain changes from end to end in a decade. According to your comments, we analyze the Miller-Tans plots every five years (2006/2010, 2011/2015, and 2016/2020) and could find out clear changing in CN and CS region. We showed all graph in Supplementary Figure S7. According to the reanalysis, we revised all manuscripts in section 3.5.

Section 3.5 from P21 L26: To understand the source regions affected AMY CH_4 level, we analysed PSS with hourly CH_4xs from 2006 to 2020. CH_4xs did not vary much and was 49 ± 74 ppb during 2006–2010 and 50 ± 70 ppb during 2016–2020. According to the PSS analysis, affecting major source regions were CN, CS and KL sectors (Fig. 9 (a)). Sources affecting CS and KL are paddy and livestock fields and that for CN was reported to be fossil fuel emissions mainly (Zhang et al., 2011, Ito et al., 2022, Chen et al., 2022).

Through the HYSPLIT cluster analysis from 2006 to 2020, we categorized the TAP $\delta^{13}C_{(CH4)}$ data and select the samples only affected by each source regions, CN, CS, and KL, respectively (section 2.6). Using TAP $\delta^{13}C_{(CH4)}$ long-term data from 2006 to 2020 affected by CN, CS and KL, Miller-Tans plots indicated that emissions from CN were mainly related to fossil fuel or biomass burning ($-44.3\pm1.8‰$), while CS ($-56.1\pm1.5‰$) and KL ($-54.6\pm1.2‰$) were affected more by biogenic sources during 2006–2020 (Fig.9 (b)). Sherwood et al. (2017) reported unweighted global mean $\delta^{13}C$ of $-44.8\pm10.7‰$ from fossil fuel use, $-26.2\pm4‰$ from biomass burning, and $-61.7\pm6.2‰$ from microbial sources. Even though the uncertainty of isotopic source signature is quite large, CH_4 formed at high temperature such as combustion is enriched in the heavier isotope while CH_4 from wetland, rice paddies and livestock is depleted. Therefore, our isotope analysis was well matched to reported source regions.

On the other hand, isotope signatures were shifted slightly in China (CN and CS) while for Korea (KL) it was steady in the uncertainty range from 2006 to 2020. When we analyze the Miller-Tans plots in every 5 years (Fig. S7), for CN the slope was -38±3‰ in 2006/10 but it became depleted -45±2.4‰ in 2016/20 while those value was enriched from -59.8±1.5‰ to -51.9±2.5‰ in CS. KL showed the quite constant values from -55 to -54‰ in the same period. This suggested that CH_4 growth rate in East Asia was affected not only biogenic but also pyrogenic sources, unlike global. The recent global accelerated increase in atmospheric CH_4 was more related to biogenic sources such as agriculture and wetland (Jackson et al., 2020, Lan et al., 2021).

Since the CH_4 emissions from agriculture and livestock accounted for 30% and 36% in China and Korea respectively in 2020 (Crippa et al., 2022), CH_4 might be increased by temperature impacts on biogenic CH_4 source. However, the fast urbanization and energy consumption strategy also can affect these regions. Especially the coal emissions decreased from 2010 in China (Liu et al., 2021) but the coal to gas policy lead natural gas consumptions increase again in China (Wang et al., 2022).

Overall, AMY and global growth rates were renewed in 2006 and during 2006–2020; the increasing trend could be linked to mixed biogenic and fossil fuel sources in East Asia while global to more biogenic sources.

Regarding this, we revised the abstract and section 4. Summary and conclusion as well.

P1 L2: From the long-term records at AMY, we confirmed that growth rate increased 3.3 ppb·yr⁻¹ during 2006/2010 and by 8.3 ppb·yr⁻¹ from 2016 to 2020, which is similar trend to global. It is reported that the recent global accelerated CH_4 growth rate was related to biogenic sources. However, isotopic signature using $\delta^{13}CH_4$ explained that CH_4 sources are becoming mixture of not only biogenic but also fossil fuel sources in East Asia from 2006 to 2020. We confirmed that long-term high-quality data can help understand changes in CH_4 emissions in East Asia.

P24 L10: From the long-term analysis of CH_4 data at AMY, average CH_4 growth rate was 3.3 ppb·yr^{-1} during 2006–2010, but increased to 8.3 ppb·yr^{-1} in 2016–2020 as similar to the global trend. Through the source distributions with our PSS analysis using CH_4xs data, CN, CS and KL sectors were main regions to affect atmospheric CH_4 observed at AMY. Isotope signature based on Miller-Tans plots at CN represents fossil fuel or burning activities while CS and KL biogenic sources during 2006-2020. However, we infer atmospheric CH_4 drivers changes in air masses arriving from China sector, CN and CS. For East Asia the increasing trend could be linked to mixed biogenic and fossil fuel sources while global to more biogenic sources (e.g. agriculture and wetland). Through this study, we confirmed that long-term high-quality data can help understand changes in CH_4 emissions in East Asia. Also, further studies are necessary based on observations to understand sources changes in East Asia since there is a discrepancy between reported inventory and observations (Wang et al., 2022).

Specific comments:

5. Page 2, line 28: "Kim et al., 2014" should be "Kim et al., 2015".

Corrected

6. Page 2, line 30-32: "Li et al., 2020" and "Li et al., 2022" are not listed in References.

Corrected

7. Page 2, line 36: "Turnbull et al., 2015" is not listed in References.

Corrected

8. Page 3, line3: "Watanabe et al. 2000" is not listed in References.

9. Page 4, line 17: What's the "−90℃" mean? If it's not the trap temperature, it should be removed to avoid confusion.

10. Page 5, line 6: I believe that the four laboratory standards are kept in high-pressure cylinders. I think that it would be better to clarify what kind of cylinders are used for the laboratory standards (volume and material).

We added the information here.

P5, L11 : They are provided with 29.5 L aluminum cylinder (Luxfer, UK) by CCL and filled with 130 bar (https://gml.noaa.gov/ccl/service.html, last access: 5 Jan.,2023). Their recalibration in every 3 years is highly recommended for CO_2, CH_4 and CO. Our laboratory standards have been recalibrated every 3 years or replaced to new sets since the first using in 2012 according to the recommendation but remaining pressure in each cylinder is still high around 100 bar.

11. Page 5, line 13-20: I'm a little bit confused by this part. I think that the CRDS analyzer (Picarro) give dry mol fractions of the atmospheric CH_4. So, why does the authors discuss the dilution effect of water vapor?

We do not use the water correction function provided by CRDS since we believe that H_2O value also should be calibrated when we apply the correction algorism to our data and general water correction cannot be applied to each instrument in different environment. In this context, many networks and stations don't use dry mole fraction reported by Picarro and apply post-processing water correction (Hazan et al., 2016, Zellweger et al.,

2016).

In our case, we don't use post-processing since we dry our samples through cryogenic method (detailed in section 2.2). Also, even when we compress air into cylinder for working standards, we dry them. However, it should be considered the bias resulted from the differences of H_2O values between samples and standards or working and laboratory standards. To avoid the confusion, we added the sentence.

P 4, L20: Despite the Picarro provides built-in dry correction algorism, this is not applied to our data since generic water correction cannot be applied to each instrument in different environment. Though we dry our samples with this system, the biases resulted from the different H_2O values between samples and standards or working and laboratory standards are considered here. This is described in section 2.3 and 3.1.

[Reference]

Hazan, L., J. Tarniewicz, M. Ramonet, O. Laurent, and A. Abbaris.: Automatic processing of atmospheric CO2 and CH4 mole frations at the ICOS Atmosphere Thematic Centre, Atmos. Meas.Tech., 9, 4719-4736, 2016

Zellweger, C., L. Emmenegger, M. Firdaus, J. Hatakka, M. Hemann, E. Kozlova, T. G. Spain, M. Steinbacher, M. V. van der Schoot, B. Buchmann.: Assessment of recent advances in measurement techniques for atmospheric carbon dioxide and methane observations, Atmos. Meas.Tech., 9, 4737-4757, 2016

12. Page 5, line 17 (Eq. 1): It should be better to clarify what the $C_{dilution}$ and C_{dry} mean. And the definition of H_{act}, "H_2O difference between standard gases and samples", is rather confusing. Is it "H_2O difference between laboratory standard gases and working standard gases"?

Agree. We corrected the sentence and added the definition.

P6, L7 where C is the CH$_4$ mole fraction and H_{act} is the actual water mole fraction (in %). Here H_{act} is the H$_2$O difference between laboratory and working standards. C_{dry} is the CH$_4$ mole fraction of laboratory standard while $C_{dilution}$ is the expected CH$_4$ mole fraction when H_{act} existed. We calculated the bias from the difference C_{dry} and $C_{dilution}$.

13. Page 7, line 10-11: It should be better to clarify the detail of the fitting function (order of polynomial and order of harmonics) and the cut-off frequency for the digital filtering based on Thoning et al. (1989).

To clarify the method, we add the explanation in Appendix B, Supplementary (and like below).

P7, L28: The details were described in Appendix B the supplementary.

APPENDIX B in Supplementary

After the baseline selection through the 3 steps (section 2.4.2), selected data are computed by curve-fitting methods. The basic components of the curve are a second-order polynomial representing the long-term trend, and a series of harmonics representing the average seasonal cycles (Eq.S1).

$$f(t) = a_0 + a_1 t + a_2 t^2 + \Sigma_{k=1}^4 \left[b_{2k-1} \sin\left(\frac{2\pi kt}{T}\right) + b_{2k} \cos\left(\frac{2\pi kt}{T}\right) \right]$$

Equation S1. Function fit

Where t is the time in days and T is 365.25 days.

And then calculate and filter the residuals of the selected daily data about the fit function. The method used is to transform the residuals into the frequency domain using a Fast Fourier Transform (FFT), apply a low pass filter function (Eq. 2) to the frequency data, and then transform the filtered data to the real domain using an inverse FFT.

$$H(f) = \exp\left[- \ln(2) * \left(\frac{f}{f_c}\right)^6\right]$$

Equation S2. Low pass filter function

Where f is frequency and fc is cut-off frequency. Here fc is cut-off values of 80 days for the short-term filter and 667 days for the long-term filter.

Finally determine the smoothed curve of interest by combining the function with the filtered data.

14. Page 7, line 12: It should be better to clarify how to compute the monthly data, long-term trend, and seasonal amplitude in detail.

The definitions are derived from Global Monitoring Laboratory - Carbon Cycle Greenhouse Gases (noaa.gov) (https://gml.noaa.gov/ccgg/mbl/crvfit/crvfit.html, last access, 16, 2023). These explanations are also included in Appendix C, the supplementary (like below).

P7, L29: Finally, we can get the L3 monthly data, long-term trend and seasonal amplitude after applying Thoning et al. (1989). The detailed definitions are in Appendix C, supplementary.

APPENDIX C in Supplementary

The definitions are derived from Global Monitoring Laboratory - Carbon Cycle Greenhouse Gases (noaa.gov) (https://gml.noaa.gov/ccgg/mbl/crvfit/crvfit.html, last access, 16, 2023).

Simply L3 monthly mean are calculated by average of daily smoothed data from Eq. S1 and Eq. S2. Daily smoothed data is the function fit plus the filtered residuals using the short term cut off (80 day/cycle)-1.

Long-term trend is upward growth in the data with the seasonal cycle removed. This is the polynomial part of the function fit plus the filtered residuals using the long-term cut-off value with (667 day/cycle)-1.

Seasonal amplitude is magnitude of the peak to trough of the detrended seasonal cycle. Detrended seasonal cycle can be obtained by subtracting the trend curve from the smooth curve.

15. Page 7, Table 2: There are no values of MS for AMY and ULD. Does it mean that MS criteria were not applied to the data for AMY and ULD?

Sorry for the confusion. The same value of MS is applied to AMY and ULD as well. We put the explanation like:

Table 2: $1.8\sigma_{30d}$ (for all three stations)

P7, L21: C is the standard deviation of 30 days moving average multiplied by α and here $1.8\sigma_{30d}$ is applied to all three stations as C.

16. Page 7, line 25-26: The geological locations of WLG and RYO are already given in page 3, line 1-3.

We deleted the explanation and used only abbreviation.

17. Page 8, line 6-8: It should be better to add the reference for the CH$_4$ isotopic measurement at INSTAAR.

We added the reference in the manuscript on page 8 line 19.

[Refence]

Miller, J. B., K. A. Mack, R. Dissly, J. W. C. White, E. J. Dlugokecky, P. P. Tans.: Development of analytical methods and measurements of 13C/12C in atmospheric CH$_4$ from the NOAA Climate Monitoring and Diagnostics Laboratory Global Air Sampling Network, J. Geophys. Res. Atmos. 107, https://doi.org/10.1029/2001JD000630, 2002

18. Page 8, line 5 and 9: It says here that the distance between TAP and AMY is 24 km. But other parts in this manuscript, the distance is 28 km. Which value is correct?

Thank you for the correction. We revised distance between TAP and AMY to 28 km through all manuscript.

19. Page 8, line 9-10: It should be better to add a figure showing synoptic scale variations of CH$_4$ observed at AMY and TAP.

We added the relevant figures in supplementary as Figure S3 and the reference in the manuscript on page 8 line 21.

P8, L21: Since TAP and AMY are only 28 km apart, their data are representative of the same region under large synoptic conditions (Fig. S3), especially for well mixed air. These data were thus used to trace the changes in the surrounding environment in East Asia (section 3.5).

20. Page 8, line 35-page 9, line 4 (2.7 PSS analysis): Since I'm not sure PSS analysis, I tried to read the cited papers, Remann et al., 2004, 2008; Li et al., 2017. But these papers are not listed in References. If the single line for each backward trajectory is used for the calculation of $C_{(i,j)}$, the sensitivity of the potential source strength increase with the distance from the start point in comparison with the reality. This effect would result in the overestimation of the potential source strength with increasing the distance from the station, wouldn't it?

I agree. As you mentioned, the potential source strength can be overestimated around the receptor site because the more trajectories pass through the grid cell i,j, as it more close to receptor site. In order to correct the overestimations, we adapted the geometric adjustment factors (Fi,j) as described by Poirot and Wishinski (1986). Calculation of adjusted residence time over each grid cell of i,j was accomplished using the following two equations:

$$T_{(i,j,a)} = \sum_{n=1}^{N} \frac{S_{(i,j,n,a)}}{V_{(n,a)}} * F_{(i,j)} \qquad \text{Eq (1)}$$

$$F_{(i,j)} = \frac{\pi\left[\left(D_{(i,j)} + \frac{d_g}{2}\right)^2 - \left(D_{(i,j)} - \frac{d_g}{2}\right)^2\right]}{d_g \times d_g} \qquad \text{Eq (2)}$$

As shown in below Illustrations of residence time calculation for a single randomly selected back-trajectory (Figure A), S(i,j,n,a) is the length of that portion of the nth segment of the a back-trajectory which falls over grid cell i,j. V(n,a) is the average speed of the air parcel

as it travels along the nth segment of the a back-trajectory. The geometric adjustment factor (Fi,j) were calculated using Equation (2). Where dg is the length of the grid cell of i,j; D(i,j) is the distance from receptor site to the grid cell of i,j.
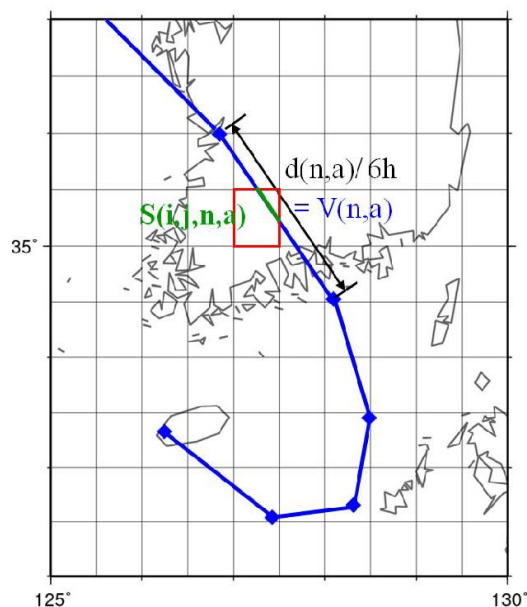

Figure A. Illustration of residence time calculation on a grid cell (i,j) of a HYSPLIT back-trajectory arrived at Jeju Gosan station.

Additionally we added missing reference and revised the manuscript like below:

Section 2.7 Potential Source Strength (PSS) analysis

To identify and illustrate the potential source distributions for regional pollutions, we calculated the PSS using the trajectory statistics approach, which has often been applied to estimate the potential source areas of greenhouse gases (Reimann et al., 2004, 2008; Li et al., 2017). The trajectory statistics approach was introduced first by Seibert et al. (1994). The underlying assumption of the method is that elevated atmospheric levels at an observation site are proportionally related to the air mass residence time on a specific grid cell over which observed air mass has been passing. Thus, this method simply calculates the airmass residence time weighted mean concentrations (here mole fractions) for target compounds (CH_4 in this study) in the domain with 0.5×0.5 grids using the following formula (Eq. 2):

$$\overline{C_{(i,j)}} = \frac{\sum_{a=1}^{M} T_{(i,j,a)} C_a}{\sum_{a=1}^{M} T_{(i,j,a)}} \qquad \text{(Eq. 2)}$$

where $C_{(i,j)}$ represents the potential source strength of the grid cell i, j as a potential source region of the target compound (CH_4); a is the index of the trajectory; M is the total number of trajectories that passed through cell i, j; C_a is the enhanced mole fraction (difference from background mole fractions mentioned in section 3.2 below) measured during the arrival of trajectory a; and $T_{(i,j,a)}$ is the residence time of trajectory a spent over grid cell i, j and which were calculated using the method described by Poirot and Wishinski (1986) as following formula (Eq.3)

$$T_{(i,j,a)} = \sum_{n=1}^{N} \frac{S_{(i,j,n,a)}}{V_{(n,a)}} \qquad \text{(Eq. 3)}$$

where $S_{(i,j,n,a)}$ is the length of that portion of the nth segment of the a back-trajectory which falls over grid cell i,j. $V_{(n,a)}$ is the average speed of the air parcel as it travels along the nth segment of the a back-trajectory. Backward trajectories were calculated using the HYSPLIT model of the NOAA Air Resources Laboratory (ARL) using meteorological information from the Global Data Assimilation System (GDAS) model. For the trajectory reliability, we used only the 4-days (96h) backward trajectories at an altitude of 500 m above the mean sea level. To consider the influence of air masses on emissions at ground level, the air masses passing above the boundary layer height (BLH) were excluded. The BLH can was obtained from the HYSPLIT model. To exclude the influences of emission sources surrounding AMY stations, enhanced CH_4 data with wind speeds lower than 2 m·s^{-1} were ruled out for the PSS analysis. When we compare PSS analysis among AMY, JGS, and ULD using CH_4xs data from 2016 to 2020, they showed the similar source regions while the coverage and CH_4xs are slightly different (Fig. S4.).

[Reference]

Poirot, R L, and Wishinski, P R. Visibility, sulfate and air mass history associated with the summertime aerosol in northern Vermont. Atmos. Environ., 20, 1457-1469, 1986

21. Page 12, line 8-9: Are the characteristics of the bivariate polar plots for the three stations (Figs. 3-5) same with those for the other years?

Yes. The reason why we showed the bivariate plots in 2018 is there was only weak typhoon, so the year of 2018 is very reasonable. We showed the example in 2019 here with sever typhoon but basically all plots show the similar characteristics which we described in the manuscript. We also revised sentence like below:

P13, L8: To understand the influence of local surface wind on observed CH_4, bivariate polar plots were used for 2018, the year less affected by typhoons compared to other years
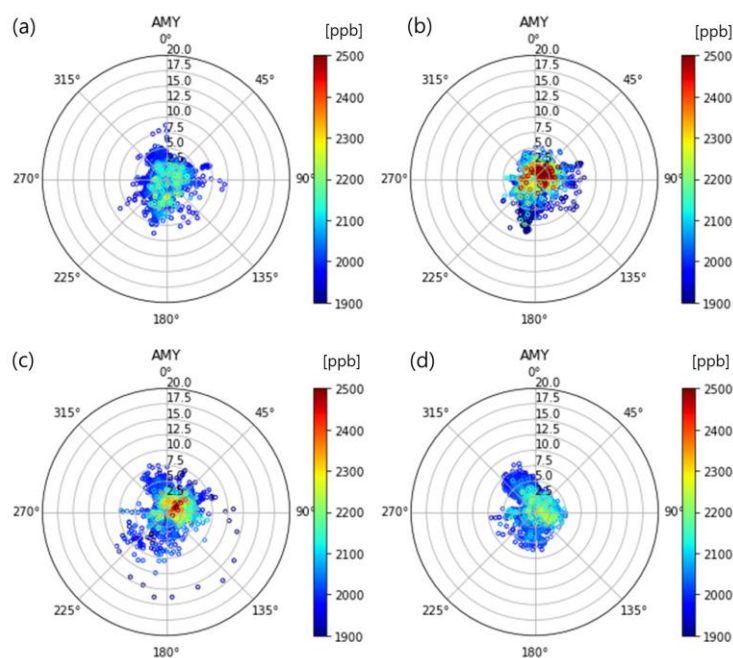

Figure A. Bivariate polar plots for observed CH_4 (L2 hourly) in spring (a), summer (b), autumn (c), and winter (d) at AMY in 2019.
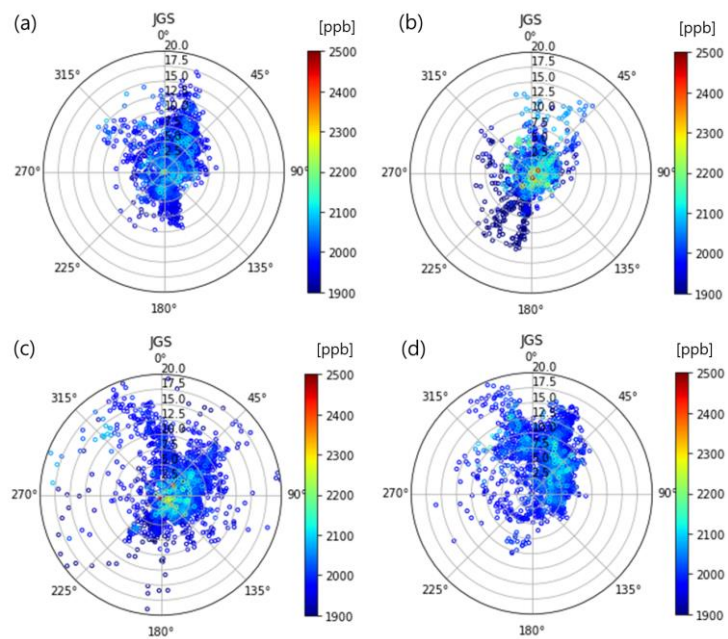
Figure B. Bivariate polar plots for observed CH$_4$ (L2 hourly) in spring (a), summer (b), autumn (c), and winter (d) at JGS in 2019.
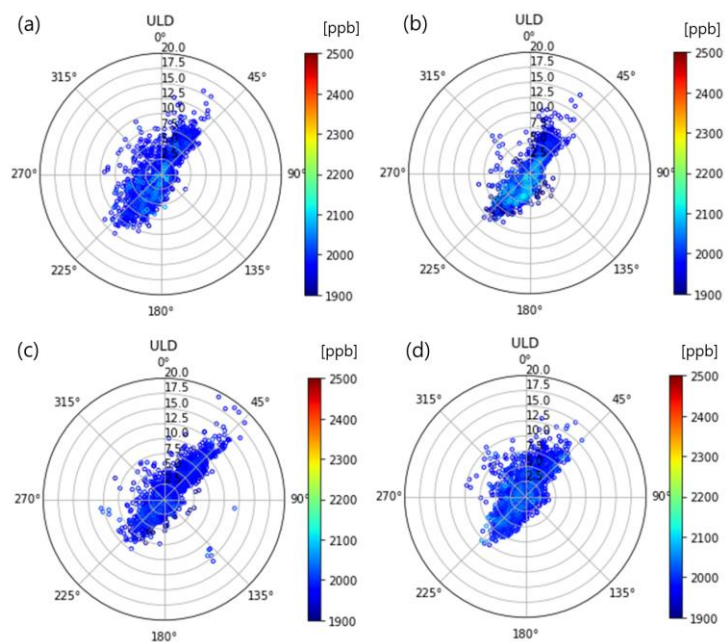

Figure C. Bivariate polar plots for observed CH$_4$ (L2 hourly) in spring (a), summer (b), autumn (c), and winter (d) at ULD in 2019.

22. Page 18, line 10-11: The seasonal cycle of the atmospheric CH$_4$ is also influenced by the atmospheric transport.

Agree. We revised the sentence here.

P19, L10: The seasonal amplitude is related to the seasonal atmospheric transport, the combination of CH$_4$ surface flux distribution and chemical loss by reactions with OH and by soil loss.

23. Page 18, line 19: The distance between TAP and AMY is repeatedly described in this manuscript.

Corrected.

24. Page 18, line 20: "during" what?

Corrected

25. Page 19, Figure 7b: Why don't the authors plot the negative growth rate in the figure?

We revised to a new graph.

26. Page 19, line 12: Was the annual growth rate calculated from the annual means based on the monthly means, listed in Table 4? If so, it would be helpful for the readers to describe that in the manuscript.

It was described in Table 4 caption, but we also explain this in section 2.4.2.

P8 L13: <mark>Annual means are averaged by monthly means while annual growth are derived from the difference of consecutive annual means.</mark>

27. Page 19, line 15: CH_4 at AMY, JGS, JLD, and RYO showed significant increases from 2016 to 2017, but small (or negative) increases from 2017 to 2018.

 Corrected

P 21 L1: Especially from 2016 to 2017, WLG showed no increase in CH_4, while CH_4 at other stations <mark>showed small or negative increases from 2017 to 2018.</mark>

28. Page 20, line 1: There is relatively large differences in the CH_4 growth rate between WLG and the WMO global mean in 2017 and 2020.

Even though they showed the value difference, the increase/decrease trend is similar. According to regions, the value of station's growth rate can be different, but the trend can be similar when they capture the baseline conditions. The growth rate value can be differed from the regions since their source and sink distributions are different at each region.

We revised the sentence to avoid confusion.

P 21 L2: <mark>Normally the growth rate in CH_4 at WLG matches well with the WMO global increase/decrease</mark> trend (Fig. 7. (b)).

29. Page 20, line 5-6: There is no description about the $\delta^{13}CH_4$ data at AMY. Please add the explanations for the data. In addition, since the plot shown in Fig. S3 is not Keeling plot but Miller-Tans plot, the slopes of the plots represent the $\delta^{13}C$ of the CH_4 sources.

Agree. We added AMY flask explanations.

P8 L22: AMY started flask sampling for CH_4 and $\delta^{13}C_{(CH4)}$ in December 2013 with same method like TAP and these data were used only for characterization of CH_4 at AMY in section 3.5.

It is typo so that we corrected it in the manuscript and the Fig. S3 (now it is Fig.S6) as well.

P21 L6: Miller-Tans plots shows the signature of CH_4 increments into background air of Mauna Loa (Fig. S6). And the slope was –52.3±2.2‰ in winter and –53.7±0.7‰ in summer at AMY during 2016 to 2020..

30. Page 21, line 1: "Sources affecting CS and KL were paddy fields and …" ?

We wrote below:

P21 L28: Sources affecting CS and KL are paddy and livestock fields and that for CN was reported to be fossil fuel emissions mainly (Zhang et al., 2011, Ito et al., 2022, Chen et al., 2022).

31. Page 21, line 13: I'm not sure what "this assumption" means.

We revised whole descriptions in section 3.5. as we described in #4 above.

32. Page 21 line 3-14: Are all the flask data collected at TAP plotted in Figs 9? Are the source regions of all the flask data classified into three sectors, CS, CN, and KL? How are they classified?

To avoid the confusion, we added detailed information.

P22 L1: Through the HYSPLIT cluster analysis from 2006 to 2020, we categorized the TAP $\delta^{13}C_{(CH4)}$ data and selected the samples only affected by each source regions, CN, CS, and KL, respectively (section 2.6).

33. Page 26, line 21-23: "Shuang-Xi et al., 2013" is not cited in the text.

corrected

34. Page 27, line 3-5: "Winderlich et al., 2010" is not cited in the text.

It was cited in p 12 line 10

Author's responses to reviewer's comments follow. A copy of the reviewer comment is given (with comment 'number') followed by a response (blue font).

Response to referee 2

1. General comment

The clear explanation of the set-up of the measurements at the 3 stations, scale propagation and uncertainty would be valuable to others developing and refining greenhouse gas measurement systems. The publication of the high-quality data from the stations, and discussion of the regional context is good. I think further work should be done on the source identification (section 3.5). This may change the overall conclusion of the work – i.e. whether the changes in the region are a relative increase in biogenic sources or not. Before publication some edits are required.

Thank you for your comments on the paper's value. We also appreciate your helpful comments to improve our manuscript. According to your specific comments, we revised our manuscript, especially isotope analysis results. Also, we tried to explain PSS analysis more detailed.

2. Isotopic signatures of source regions

The section on the isotopic signatures for identifying the predominant sources is interesting but needs some more work: The Keeling plot technique (δ 13C against 1/CH4) is only appropriate for a constant background. Some detail is required about how these Keeling plots were constructed. Is a constant background appropriate or are you plotting data over a period when there will be seasonal variability or interannual differences in the background? If you are plotting data over several years and the global background methane mole fraction and δ 13C are changing, then Keeling plots should not be used. If the constant background assumption cannot be made then Miller-Tans plots could be used instead to identify the source isotopic composition, e.g.

Miller and Tans, 2003 https://doi.org/10.1034/j.1600- 0889.2003.00020.x; Al-Shalan et al., 2022 https://doi.org/10.1016/j.atmosenv.2021.118763; Varga et al., 2021. Figure 9 In (c) and (d) we see that source signatures for CS and KL increased in 2016-2020 compared with 2006-2010. This seems to contrast with line 13 on page 21 which talks of a decreasing trend in δ 13C What are the uncertainties in the trends in (e) and (f). Can you really say there is a trend?

Agree. According to your comments, we analysed the Miller-Tans plot and could get more clear results for source changes. So we use PSS analysis as a tool to show the representative area where affected atmospheric CH$_4$ at AMY. Through the HYSPLIT cluster analysis based on TAP flask sampling dates, we selected the samples from the source regions where PSS analysis indicated. Miller-Tans plots were analysed every five years to see its changes.

Finally, we revised whole description in section 3.5. like below and we also added new graph in the manuscript and supplementary:

Section 3.5 from P21 L26: To understand the source regions affected AMY CH$_4$ level, we analysed PSS with hourly CH$_4$xs from 2006 to 2020. CH$_4$xs did not vary much and was 49 ± 74 ppb during 2006–2010 and 50 ± 70 ppb during 2016–2020. According to the PSS analysis, affecting major source regions were CN, CS and KL sectors (Fig. 9 (a)). Sources affecting CS and KL are paddy and livestock fields and that for CN was reported to be fossil fuel emissions mainly (Zhang et al., 2011, Ito et al., 2022, Chen et al., 2022).

Through the HYSPLIT cluster analysis from 2006 to 2020, we categorized the TAP $\delta^{13}C_{(CH4)}$ data and select the samples only affected by each source regions, CN, CS, and KL, respectively (section 2.6). Using TAP $\delta^{13}C_{(CH4)}$ long-term data from 2006 to 2020 affected by CN, CS and KL, Miller-

Tans plots indicated that emissions from CN were mainly related to fossil fuel or biomass burning (–44.3±1.8‰), while CS (–56.1±1.5‰) and KL (– 54.6±1.2‰) were affected more by biogenic sources during 2006–2020 (Fig.9 (b)). Sherwood et al. (2017) reported unweighted global mean $\delta^{13}C$ of –44.8±10.7‰ from fossil fuel use, –26.2±4‰ from biomass burning, and –61.7±6.2‰ from microbial sources. Even though the uncertainty of isotopic source signature is quite large, CH_4 formed at high temperature such as combustion is enriched in the heavier isotope while CH_4 from wetland, rice paddies and livestock is depleted. Therefore, our isotope analysis was well matched to reported source regions.

On the other hand, isotope signatures were shifted slightly in China (CN and CS) while for Korea (KL) it was steady in the uncertainty range from 2006 to 2020. When we analyze the Miller-Tans plots in every 5 years (Fig. S7), for CN the slope was -38±3‰ in 2006/10 but it became depleted -45±2.4‰ in 2016/20 while those value was enriched from -59.8±1.5‰ to -51.9±2.5‰ in CS. KL showed the quite constant values from -55 to -54‰ in the same period. This suggested that CH_4 growth rate in East Asia was affected not only biogenic but also pyrogenic sources, unlike global. The recent global accelerated increase in atmospheric CH_4 was more related to biogenic sources such as agriculture and wetland (Jackson et al., 2020, Lan et al., 2021).

Since the CH_4 emissions from agriculture and livestock accounted for 30% and 36% in China and Korea respectively in 2020 (Crippa et al., 2022), CH_4 might be increased by temperature impacts on biogenic CH_4 source. However, the fast urbanization and energy consumption strategy also can affect these regions. Especially the coal emissions decreased from 2010 in China (Liu et al., 2021) but the coal to gas policy lead natural gas consumptions increase again in China (Wang et al., 2022).

Overall, AMY and global growth rates were renewed in 2006 and during 2006–2020; the increasing trend could be linked to mixed biogenic and fossil fuel sources in East Asia while global to more biogenic sources.

Regarding this, we revised the abstract and section 4. Summary and conclusion as well.

P1 L2: From the long-term records at AMY, we confirmed that growth rate increased 3.3 ppb·yr^{-1} during 2006/2010 and by 8.3 ppb·yr^{-1} from 2016 to 2020, which is similar trend to global. It is reported that the recent global accelerated CH_4 growth rate was related to biogenic sources. However, isotopic signature using $\delta^{13}CH_4$ explained that CH_4 sources are becoming mixture of not only biogenic but also fossil fuel sources in East Asia from 2006 to 2020. We confirmed that long-term high-quality data can help understand changes in CH_4 emissions in East Asia.

P24 L10: From the long-term analysis of CH_4 data at AMY, average CH_4 growth rate was 3.3 ppb·yr^{-1} during 2006–2010, but increased to 8.3 ppb·yr^{-1} in 2016–2020 as similar to the global trend. Through the source distributions with our PSS analysis using CH_4xs data, CN, CS and KL sectors were main regions to affect atmospheric CH_4 observed at AMY. Isotope signature based on Miller-Tans plots at CN represents fossil fuel or burning activities while CS and KL biogenic sources during 2006-2020. However, we infer atmospheric CH_4 drivers changes in air masses arriving from China sector, CN and CS. For East Asia the increasing trend could be linked to mixed biogenic and fossil fuel sources while global to more biogenic sources (e.g. agriculture and wetland). Through this study, we confirmed that long-term high-quality data can help understand changes in CH_4 emissions in East Asia. Also, further studies are necessary based on observations to understand sources changes in East Asia since there is a discrepancy between reported inventory and observations (Wang et al., 2022).

3. References

The reference lists need editing. Some of the references were missing from the reference list: Watanabe et al., 2000; Remann et al., 2004; Remann et al., 2008; Li et al., 2017; Turnbull et al., 2015. The reference Shuang-Xi Fang et al. (2013) should be

deleted as this is already listed as Fang et al., 2013. Kim et al., 2014 on page 2 should be Kim et al., 2015 to match the reference list.

Corrected

4. Other questions:

4.1 As AMD is affected by local sources it would be helpful to use an inventory to suggest quantitatively what the anthropogenic emissions sources are (e.g. EDGAR, or UNFCCC) in the introduction.

We added the information of anthropogenic source in Korea in the introductions with the reference of EDGAR.

P 2, L10: China has also the largest anthropogenic CH_4 emissions in the world mainly from solid fuel (34%), rice cultivations (20%) and enteric fermentation (10%), respectively (Janssens-Maenhout et al., 2019; Crippa et al., 2022).

P 2, L14: South Korea major CH_4 emissions are derived from wastewater treatment (40%), enteric fermentation (22%) and then rice cultivations (14%) respectively (Crippa et al., 2022).

4.2 Figure 1 – add a scale bar to this map.

Corrected

4.3 What was the reason for drying the air rather than using the water correction built into Picarro software (see Rella et al., 2013)?

We do not use the water correction function provided by CRDS since we believe that H_2O value also should be calibrated when we apply the correction algorism to our data and general water correction cannot be applied to each instrument in different environment. In this context, many networks and stations don't use dry mole fraction

reported by Picarro and apply post-processing water correction (Hazan et al., 2016, Zellweger et al., 2016).

In our case, we don't use post-processing since we dry our samples through cryogenic method (detailed in section 2.2). Also, even when we compress air into cylinder for working standards, we dry them. However, it should be considered the bias resulted from the differences of H_2O values between samples and standards or working and laboratory standards. To avoid the confusion, we added the sentence.

P 4, L20: Despite the Picarro provides built-in dry correction algorism, this is not applied to our data since generic water correction cannot be applied to each instrument in different environment. Though we dry our samples with this system, the biases resulted from the different H_2O values between samples and standards or working and laboratory standards are considered here. This is described in section 2.3 and 3.1.

[Reference]

Hazan, L., J. Tarniewicz, M. Ramonet, O. Laurent, and A. Abbaris.: Automatic processing of atmospheric CO2 and CH4 mole frations at the ICOS Atmosphere Thematic Centre, Atmos. Meas.Tech., 9, 4719-4736, 2016

Zellweger, C., L. Emmenegger, M. Firdaus, J. Hatakka, M. Hemann, E. Kozlova, T. G. Spain, M. Steinbacher, M. V. van der Schoot, B. Buchmann.: Assessment of recent advances in measurement techniques for atmospheric carbon dioxide and methane observations, Atmos. Meas.Tech., 9, 4737-4757, 2016

4.4 Page 2, line 31. A large ratio, CH4/C2H6 – explain what that means. Is high methane but low ethane indicative of a biogenic source?

We explicitly explained what it means.

: The ratio, CH_4/C_2H_6, was observed 53 ppb·ppb^{-1} during KORUS-AQ campaign from May to June 2016 which seems to be associated fossil fuel in Seoul and Busan while it was 150 to 250 ppb·ppb^{-1} related to biogenic emissions such as rice paddies in southern western part of South Korea (Li et al., 2022).

4.5 Page 3 – lines 29/30. Were there 2 garbage incinerators or one? This part needs clarifying.

Thank you for the correction. We revised the sentence.

P3 L31: In the southwestern area, there is a small brickyard 200 m from the station and a garbage incinerator within 100 m. The garbage incineration facility was moved to the north side of island in December 2016.

4.6 Page 7 – it's not clear how the filtering was applied to the data using HS, CD and MS. Are data outside of 1 s.d. of the mean filtered out?

Since this method was published in Seo et al.(2021), we did not handle this process precisely. However, we tried to explain our method with more clear ways here to avoid the confusions.

P7 L14 There are three steps to select the background levels (L3 hourly data) from valid L2 hourly data:

Step 1) $HS(t) \leq A$

Step 2) $| HA(t) - HA(t - 1)| \leq B$ or $|HA(t) - HA(t + 1) | \leq B$

Step 3) $| HA(t) - 30$ days moving median of of HA $| \leq C.$

Where HS represents CH_4 hourly standard deviation, HA is CH_4 hourly means and t represents time in hours. In step 3), t is the middle of the time window. A, B and C are criteria determined empirically for each step, as given in Table 2. C is the standard deviation of 30 days moving average multiplied by α and here $1.8\sigma_{30d}$ is applied to all three stations as C.

Even though the data were selected by step 1) and 2), high CH_4 levels remained because of long-lasting stagnant conditions (e.g. over 6 days). Therefore, we also apply step 3). This process retained 21–52% of the data at each station, which were defined as L3 hourly on observations (Fig. S2). To get L3 daily/monthly data, the method developed by Thoning et al. (1989) was used to fit smooth curves to the daily averages computed by L3 hourly data. The methods reduce noise induced by synoptic-scale atmospheric variability, fill measurement gaps, and are used to represent the regional baseline. The details were described in Appendix B the supplementary. Finally, we can get the L3 daily data, L3 monthly data, long-term trend and seasonal amplitude after applying Thoning et al. (1989). The detailed definitions are in Appendix C, supplementary.

We also revised the table 2 and added the supplementary figure (Figure S2) to show our method.

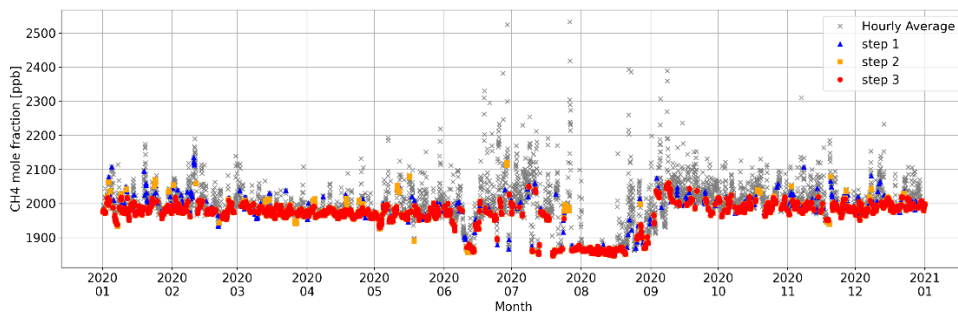Table 2. Criteria and percentage of selected background levels from observed data at each station.

Station ID	AMY	JGS	ULD
Data period	1999 to 2020	2012 to 2020	2012 to 2020
A [ppb]	2.1	2.1	2.8
B [ppb]	4.9	5.2	3.6
C [ppb]	$1.8\sigma_{30d}$ (for all three stations)		
Spring, MAM [%]	29.1	46.6	57.9
Summer, JJA [%]	11.0	33.5	37.6

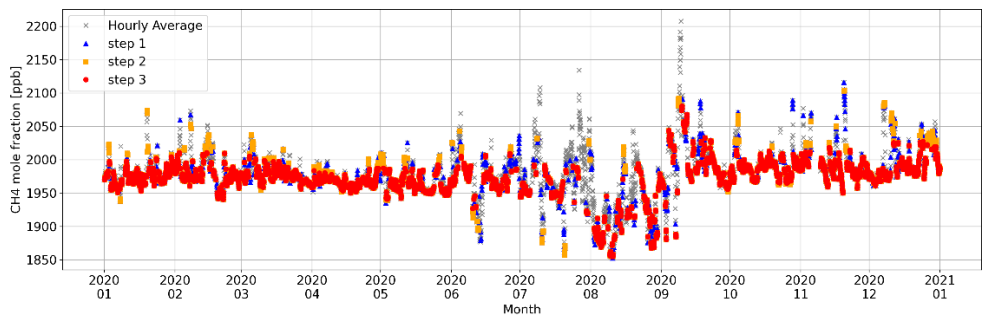|			
Autumn, SON [%]	16.9	30.9	53.2
Winter, DJF [%]	28.4	49.1	58.9
Total [%]	21.3	40.64	52.2

(a)
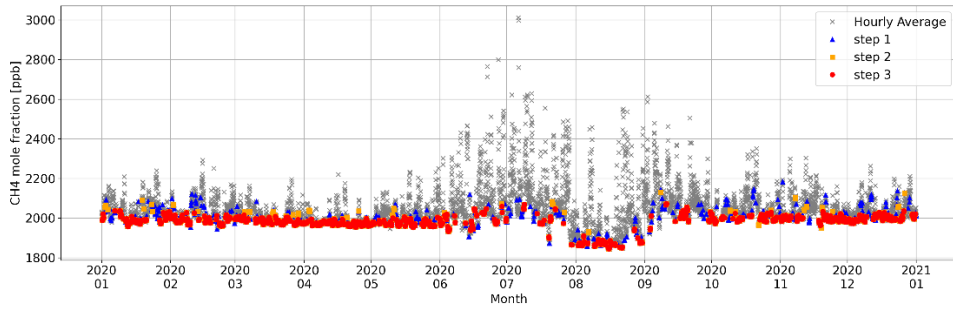
(b)

(c)

Figure S2. The time series of hourly CH$_4$ data through our selection method from step 1 to 3 at (a) AMY (b) JGS and (c)ULD in 2020.

4.7 Page 8 – line 15 – typo in HYSPLIT

Corrected

4.8 Figure 7 – The growth rates for AMY, JGS and ULD aren't shown for 2018. I think this is because they are negative (-1 ppb) but this is still a result so they should be shown.

Corrected

4.9 Why are some of the numbers in Table 4 written in bold?

Corrected

4.10   Figure 8 – 2009 was unusual because there was no seasonal cycle – can you comment on why this was?

When we reviewed the raw, L1 and L2 data, other period captured the summer drop but 2009 had an instrumental issue in summer. We commented in the manuscript.

P21 L20: In 2009 there is no clear seasonal cycle. There was an instrumental issue in summer while other period captured summer drop by observations.

4.11   I didn't fully understand the PSS analysis – I think that needs some more detail

To explain PSS analysis in detailed we revised the section 2.7.

Section 2.7: To identify and illustrate the potential source distributions for regional pollutions, we calculated the PSS using the trajectory statistics approach, which has often been applied to estimate the potential source areas of greenhouse gases (Reimann et al., 2004, 2008;

Li et al., 2017). The trajectory statistics approach was introduced first by Seibert et al. (1994). The underlying assumption of the method is that elevated concentrations at an observations site are proportionally related to the air mass residence time on a specific grid cell over which observed air mass has been passing. Thus, this method simply calculates the airmass residence time weighted mean concentrations for target compounds (CH_4 in this study) for the domain with 0.5×0.5 grids using the following formula (Eq. 2):

$$\overline{C_{(i,j)}} = \frac{\sum_{a=1}^{M} T_{(i,j,a)} C_a}{\sum_{a=1}^{M} T_{(i,j,a)}} \qquad \text{(Eq. 2)}$$

where $C_{(i, j)}$ represents the potential source strength of the grid cell i, j as a potential source region of the target compound (CH_4); a is the index of the trajectory; M is the total number of trajectories that passed through cell i, j; C_a is the enhanced mole fraction (difference from background mole fractions mentioned in section 3.2 below) measured during the arrival of trajectory a; and $T_{(i,j,a)}$ is the residence time of trajectory a spent over grid cell i, j and which were calculated using the method described by Poirot and Wishinski (1986) as following formula (Eq.3)

$$T_{(i,j,a)} = \sum_{n=1}^{N} \frac{S_{(i,j,n,a)}}{V_{(n,a)}} \qquad \text{(Eq. 3)}$$

where $S_{(i,j,n,a)}$ is the length of that portion of the nth segment of the a back-trajectory which falls over grid cell i,j. $V_{(n,a)}$ is the average speed of the air parcel as it travels along the nth segment of the a back-trajectory. Backward trajectories were calculated using the HYSPLIT model of the NOAA Air Resources Laboratory (ARL) using meteorological information from the Global Data Assimilation System (GDAS) model. For the trajectory reliability, we used only the 4-days (96h) backward trajectories at an altitude of 500 m above the mean sea level. To consider

the influence of air masses on emissions at ground level, the air masses passing above the boundary layer height (BLH) were excluded. The BLH can was obtained from the HYSPLIT model. To exclude the influences of emission sources surrounding AMY stations, enhanced CH_4 data with wind speeds lower than 2 m·s^{-1} were excluded from the PSS analysis. When we compare PSS analysis among AMY, JGS, and ULD using CH_4xs data from 2016 to 2020, they showed the similar source regions while the coverage and CH_4xs are different (Fig. S5.).